

1 ORIGINAL RESEARCH

2 Short running header: Fiber-reinforced PTMC composite for osteogenic molecules delivery

3 Xi Zhang et al

4

5 **A drug eluting poly(trimethylene carbonate)/poly(lactic acid)**
6 **reinforced nanocomposite for the functional delivery of**
7 **osteogenic molecules**

8 Xi Zhang^{1,2}

9 Mike A. Geven³

10 Xinluan Wang⁴

11 Ling Qin⁴

12 Dirk W. Grijpma³

13 Ton Peijs¹

14 David Eglin⁵

15 Olivier Guillaume^{5,*}

16 Julien E. Gautrot^{1, 2,*}

17

18 ¹ School of Engineering and Materials Science, Queen Mary University of London, Mile End
19 Road, London E1 4NS, UK

² Institute of Bioengineering, Queen Mary University of London, Mile End Road, London E1 4NS, UK

³ Department of Biomaterials Science and Technology, University of Twente, P. O. Box 217, 7500 AE, Enschede, the Netherlands

⁴ Translational Medicine R&D Center, Institute of Biomedical and Health Engineering, Shenzhen Institutes of Advanced Technology, Chinese Academy of Sciences, Shenzhen 5018057, China

⁵ AO Research Institute Davos, Clavadelerstrasse 8, CH7270, Davos, Switzerland

*Correspondence: Julien Gautrot

School of Engineering and Materials Science, Queen Mary University of London, Mile End Road, London E1 4NS, UK

Email j.gautrot@qmul.ac.uk

Olivier Guillaume

AO Research Institute Davos, Clavadelerstrasse 8, CH7270, Davos, Switzerland

Email olivier.guillaume@aofoundation.org

Abstract: Poly(trimethylene carbonate) (PTMC) has wide biomedical applications in the field of tissue engineering, due to its biocompatibility and biodegradability features. Its common manufacturing involves photo-fabrication, such as stereolithography (SLA), which allows for the fabrication of complex and controlled structures. Despite the great potential of SLA-fabricated scaffolds, very few examples of PTMC-based drug delivery systems fabricated using photo-fabrication can be found ascribed to light-triggered therapeutics instability, degradation, side reaction, binding to the macromers, etc. These concerns severely restrict the development of SLA-fabricated PTMC structures for drug delivery purposes. In this context, we propose here as proof of concept, to load a drug model (dexamethasone) into electrospun fibers of poly(lactic acid) (PLA), and then to integrate these bioactive fibers into the photo-crosslinkable resin of PTMC to produce hybrid films. Such polymer/polymer hybrids exhibit advanced properties compared to PTMC-only films, in terms of mechanical performance and drug protection from UV-denaturation. We further validated that the dexamethasone preserved its biological activity even after photoreaction within the PTMC/PLA hybrid structures by investigating bone marrow mesenchymal stem cells proliferation and osteogenic differentiation. This work opens the field to drug loaded polymer/polymer composite structures obtained using photo-crosslinking for additive manufacturing processes such as stereolithography.

Key words:

fiber reinforced composite, poly(trimethylene carbonate), photo-crosslinking, dexamethasone, osteogenic materials.

1 **Introduction**

2 Poly(trimethylene carbonate) (PTMC) is a biocompatible and degradable
3 polymeric material that can be synthesized via the ring-opening reaction of 1,3-
4 trimethylene carbonate.¹ Its degradation, mediated by a surface-erosion
5 mechanism, is characterized by an extremely low level of non-enzymatic
6 hydrolysis and by the release of non-acidic by-products, which makes PTMC an
7 attractive material as polyester alternative for medical applications.^{2,3} However,
8 PTMC is usually considered to have poor mechanical performance, which restricts
9 its applications, in particular for tissue scaffolding. Several strategies have been
10 developed to improve the mechanical properties of PTMC, by increasing molecular
11 weight,⁴ blending with stiffer polymers or inorganic particles,⁵⁻⁷ copolymerizing
12 with ‘hard’ polymer blocks⁸ or crosslinking.⁹ Recently, Schüller-Ravoo *et al*
13 synthesized three-armed PTMC methacrylate macromers that can be photo-
14 crosslinked to produce flexible and tear-resistant elastomeric materials.¹⁰ In
15 addition, the ability to photo-initiate crosslinking permits the use of
16 stereolithography (SLA), a common additive manufacturing technique, to build
17 PTMC-based structures with excellent degree of precision in the control of three-
18 dimensional architectures.¹¹⁻¹³

19 An interesting feature of the slow surface degradation and erosion profile of PTMC
20 based materials is that they allow good control of the release profile of drugs in
21 presence of enzymes (such as lipases).¹⁴⁻¹⁶ Despite the potential of SLA-fabricated
22 scaffolds, very few examples of PTMC drug delivery systems fabricated using
23 photo-fabrication can be found in the literature.¹⁴ A major inconvenient of SLA, in

designing drug-loaded scaffolds, is that UV irradiation and radical generation can result in the degradation or reactivity of the drug being encapsulated, often at relatively low concentrations. Indeed, SLA requires successive layer-by-layer photoreactions of the methacrylate macromers. This intrinsically restricts the potential of SLA-fabricated scaffolds to be used as drug delivery carrier, due to radical-mediated chemical cross-reactions and due to the light sensitivity of the majority of therapeutic compounds. So far, only Vitamin B12 (as model) has been incorporated into PTMC photo-crosslinkable matrix, under the form of non-soluble micro-granules to prevent any degradation.¹⁴ In order to confer bioactive properties to SLA-fabricated PTMC scaffolds, we recently reported the incorporation of hydroxyapatite (HA) nanoparticles into the PTMC-based photo-crosslinkable resins. The composite PTMC-HA scaffolds successfully stimulated bone formation in a calvarial defect model in rabbit.¹¹ Nevertheless, a high loading of HA particles up to 40 weight % was required to elicit beneficial osteogenic effects, which renders the resin highly viscous and difficult to process for SLA-based additive manufacturing. As alternative, we further developed composite PTMC structures with enhanced mechanical properties, by incorporating electrospun poly(lactic acid) (PLA) fibers in methacrylate-terminated PTMC macromers followed by UV crosslinking.¹⁷ The improvement in PTMC mechanical performance combined with its potential bioactive and shape memory properties¹⁸ has brought interests in designing drug delivery systems that can further enhance bioactivity, in particular osteogenicity.

Dexamethasone (Dexa) is an ideal drug candidate for such applications as it is widely used *in vitro* and *in vivo* to regulate osteodifferentiation.^{19,20} Dexa is a

synthetic glucocorticoid with several therapeutic applications, such as anti-inflammatory, immunosuppressant and decongestant.²¹ It also displays potent effects on the proliferation and osteogenic differentiation of mesenchymal stem cells (MSCs) in presence of β -glycerol phosphate and ascorbic acid/ascorbate,^{22,23} with optimal concentrations ranging from 10 to 100 nM.²⁴ Similarly, icaritin is a metabolite of the flavonoid glycoside extracted from *Herba Epimedii*, which was reported to enhance the differentiation and proliferation of osteoblasts.²⁵

Various systems have been developed as Dexamethasone carriers, allowing a sustained release, such as implant dispensers,²⁶ nanoparticles/hydrogel complexes,²⁷ self-assembled nanofibrous gels,²⁸ electrospun fibers,²⁹ macroporous scaffolds³⁰ and extrusion-based structures.²⁴ Among those, Dexamethasone-charged nanoparticles can easily be administered but have low drug loading efficiency. It is also difficult to prevent their dispersion in the body following their administration for local treatment. Hydrogel/fiber composites are more suitable for local delivery and showed controlled release profiles, but their poor mechanical performance restricts their potential applications. Electrospun polymer nanofibers have gained significant interest for drug encapsulation, due to their ease of fabrication, high drug incorporation efficiency, large surface area and the inherent porosity of the scaffolds they form.³¹ However, a burst release usually occurs as a result of drug accumulation on the fiber surface and the high surface area of these materials.^{32,33} The initial burst release can be alleviated by improving drug-polymer compatibility and drug solubility in polymer solution during electrospinning (*i.e.* employing surfactants, although often by compromising cytotoxicity). A sustained release can also be achieved by fabricating complex materials that encapsulate drugs in a core-

1 shell structure, modifying fiber's chemical properties or using drug-binding
2 agents.³⁴⁻³⁸ However, these approaches considerably increase the complexity of the
3 processing methodologies and require novel chemical functionalisation that may
4 prevent regulatory approval and clinical translation.

5 The objective of our work was to fabricate PTMC/PLA nanofiber composite
6 systems (based on fibers with diameters in the micron range and below), allowing
7 the control of the release of model drugs promoting osteogenic differentiation *in*
8 *vitro*, Dexa and icaritin. PLA was selected for the fabrication of electrospun fibers
9 since it is commercially available, biocompatible, degradable, FDA approved and
10 significantly stiffer than PTMC (to achieve reinforcement). In addition to
11 composite formulation, PLA has also been routinely used to modify the physical
12 properties of degradable polymers, by copolymerizing with other monomers.³⁹ In
13 addition, combination with the PTMC matrix also improves the ductility of brittle
14 PLA fibre materials¹⁷ and confers shape memory properties, as previously reported
15 by our group.¹⁸ PLA fibers loaded with Dexa were electrospun and incorporated
16 into a photo-cured PTMC matrix. In addition to mechanical reinforcement, our
17 results demonstrate the preservation of the drug activity and the control of its
18 diffusion, compared to a direct drug-loaded PTMC strategy. In order to validate
19 this approach, the biological activity of Dexa-loaded PTMC-PLA films was
20 assessed by investigating their osteogenic properties on human mesenchymal stem
21 cells.

22 The ability to generate mechanically enhanced photo-cured PTMC composites able to
23 release active therapeutics constitutes an important progress in the use of these materials
24 for additive manufacturing and tissue engineering applications.

1

2 **Materials and methods***Materials*

3 Poly(lactic acid) (PLA 2002D, M_w 200,000 g/mol, density 1.24 g/cm³) was obtained from
4 Natureworks. PTMC (three-armed methacrylate-ended, M_n 10,000 g/mol) macromer was
5 synthesized as previously reported.⁴⁰ Chloroform, dimethylformamide (DMF), methanol,
6 dichloromethane, ethyl acetate, acetic acid, tetrahydrofuran and acetonitrile (HPLC grade)
7 were obtained from Fisher Scientific. Poly(ethylene glycol) methacrylate (average M_n
8 360 g/mol), Dexamethasone (Dexa), 2-Hydroxy-4'-(2-hydroxyethoxy)-2-
9 methylpropiophenone (Irgacure 2959, I2959), triethylamine were purchased from Sigma-
10 Aldrich. Icaritin was obtained from Shenzhen Institutes of Advanced Technology,
11 Chinese Academy of Sciences. Phosphate buffered saline was prepared by dissolving one
12 tablet (Sigma-Aldrich) in 200 ml deionized water. All materials and reagents were used
13 as received.

14 ***Electrospinning and composites preparation***

15 The electrospinning was performed using an in-house-built electrospinning system.
16 To spin PLA and icaritin/Dexa-loaded PLA fibers, a PLA solution at concentration
17 of 9 wt% in chloroform/DMF (chloroform/DMF=3/1) was firstly prepared. For
18 icaritin-loaded/low Dexa loading fibers, 0.50 wt% of icaritin/0.68 wt% of Dexa
19 (with respect to PLA) was added to the PLA solution respectively. They were
20 stirred until fully dissolved. For higher Dexa loaded fibers (2.42 wt% with respect
21 to PLA), methanol was used to replace DMF while preparing PLA solution in order
22 to increase the drug solubility. The ratio of chloroform/methanol was set at 3/1.

The PLA or PLA-Dexa solution was supplied through a PTFE tube at 1.0 mL/h to the electrospinning spinneret. The spinning was carried out at voltage of 18-20 kV and a distance of 15 cm. Random fiber mats were collected on a grounded aluminium foil sheet. Finally four different fiber mats (neat PLA fiber mats (PLA 0), PLA-icaritin fiber mats, PLA-low Dexa fiber mats (PLA 1) and PLA-high Dexa fiber mats (PLA 2)) were obtained and they were evaporated in vacuum desiccator for 48 h to remove residual solvent.

A hot-press was used to incorporate electrospun fibers into the PTMC matrix. To perform hot-pressing, PTMC macromer was first dissolved in dichloromethane at 50 wt% concentration together with 0.67 wt% of Irgacure 2959 (I2959, low cytotoxicity photoinitiator,⁴¹ with respect to PTMC). After dissolution, the PTMC/dichloromethane solution was transferred into a vacuum desiccator for 48 h to remove the dichloromethane. The dried PTMC/I2959 mixture was then ready to use for hot-pressing (Collin P300E). 40 mg of PLA fibers mat with a size of 50×50×0.08 mm, called PLA 0, PLA 1 and PLA 2, for PLA loaded with 0, 0.68 and 2.42 wt% of Dexa respectively, was placed in a 60×60×0.15 mm mould, which was then transferred into the hot-press. 160 mg PTMC macromer (containing I2959) was placed on top of the fiber mat. Fibers and PTMC were pre-warmed at 60°C for 5 min and then pressed under 25 bar pressure. A compressed film of 0.06 mm thickness was removed from the mould after cooling to room temperature. This was followed by exposing the resulting composite films under UV irradiation (Omnicure 1500) for 100 s at 15 mW/cm² to cure the PTMC macromer. The composite films were then stored in a nitrogen box prior to further characterisation and experiments. For comparison, PTMC samples without fibers were prepared by

casting PTMC/I2959 dichloromethane solution in 50×5×1 mm mould followed by evaporating solvent. PTMC was UV-cured using the same parameters as described above. Four different groups of samples were prepared, named PTMC (for PTMC without any integrated PLA fiber), PTMC/PLA 0, PTMC/PLA 1 and PTMC/PLA 2 for composite PTMC matrix integrating PLA fibers loaded with 0, 0.68 and 2.42 wt% of Dexa respectively.

Electrospun fiber and PTMC/fiber composites characterization

The morphology of electrospun fibers and PTMC/PLA fiber composites were characterized using scanning electron microscopy (SEM, FEI Inspect F). All samples were mounted onto SEM specimen stubs and sputter-coated with a thin gold layer for contrast. To investigate PTMC infiltration and PTMC-fiber interaction, composites samples were cold-fractured in liquid nitrogen and the fracture surface was characterized using SEM. Thermal properties of electrospun fibers were measured using differential scanning calorimetry (DSC, PerkinElmer DSC 4000). Samples were first equilibrated at 25°C and then ramped to 180°C at 10 °C/min. Glass transition temperature (T_g) was determined by the mid-point of glass transition. The crystallinity of PLA was calculated by,

$$X_c = \frac{\Delta H_m}{\Delta H_{ref}} \times 100\%$$

where X_c is the crystallinity, ΔH_m is the experimental heat of fusion at melting point determined by DSC, ΔH_{ref} is the theoretical heat of fusion of fully crystalline PLA (93 J/g).⁴² Tensile tests of electrospun fiber mat and PTMC/PLA fiber composites were performed using dynamic mechanical test (DMA, TA Q800) in controlled

force mode. Samples were cut into 20×5×0.06 mm rectangular strips before being mounted into the clamps. A preload force of 0.05 N was applied and specimen were stretched at 0.1 N/min rate until failure at room temperature. The Young's modulus was derived from the slope of stress-strain curve at low strain (2 %) and three tests were performed on each sample.

Gel permeation chromatography analyses

Gel permeation chromatography (GPC) was employed to investigate the possible coupling between Dexa and the methacrylate-ended PTMC macromers, in the presence of photoinitiator, during UV curing. We examined the refractive index (RI) signal of methacrylate and Dexa before and after UV curing. Instead of PTMC-methacrylate, a model of macromer PEG-methacrylate was used and dissolved in tetrahydrofuran (THF) at concentration of 2.0 mg/mL. Dexa and I2959 were added at 0.20 mg/mL and 0.17 mg/mL, respectively. The solution was degassed with nitrogen for 30 min and divided into two portions, one of which was UV treated at 15 mW/cm² for 100 s and the other not. For reference, THF solutions of Dexa and I2959 were also tested separately to identify their signals. The GPC tests were performed using Agilent Technologies 1260 infinity equipped with UV detector at 308 nm wavelength. Tetrahydrofuran (with 2.0 vol% triethylamine) was used as the eluent at a flow rate of 1.0 mL/min.

In vitro measurement of icaritin and Dexamethasone release

The amount of icaritin released in phosphate-buffered saline (PBS) was calculated by measuring the remaining icaritin in samples using high performance liquid chromatography (HPLC, Waters e2695) equipped with UV detector and a Kinetex

column (Phenomenex, C18, 100 Å, 5 µm, 150×4.6 mm). The mobile phase was 25/75 (v/v) water/acetonitrile, eluted at 1.0 mL/min, with water phase adjusted to pH 4 by adding 0.5 vol% of acetic acid and 0.3 vol% triethylamine. The test was performed at 360 nm UV adsorption wavelength with 20 µL injection. Electrospun PLA fiber mats were cut into 10×10 mm specimens and immersed in 10 mL PBS. At different time intervals, specimens were removed from PBS, rinsed with deionised water and extracted using ethyl acetate. The extractant (ethyl acetate) was evaporated and re-dissolved in methanol and analysed using HPLC (n=3 per group). Dexa concentration in PBS was analysed using the same HPLC equipment described above. The mobile phase was 50/50 (v/v) acetonitrile/PBS, eluted at 1.0 mL/min. The test was performed at 256 nm UV adsorption wavelength with 50 µL injection for each solution. To evaluate the Dexa elution from electrospun PLA fibers and PTMC/PLA fiber composites, 15×15 mm specimens were cut out from each sample and immersed in 3 mL PBS into incubator at 37°C for a period of five weeks. At different time points, each specimen was removed from the media and transferred into 3 mL fresh PBS. The recovered media was then analysed using HPLC (n=3 per group).

Cell culture and differentiation assays

PTMC/PLA fiber composite films (PTMC/PLA 0, 1 and 2) were punched into discs with diameter of around 6.0 mm (each disk weighs around 1.5 mg). The disks were then placed in 96-well plate and sterilized in ethanol 70% for 10 min.

Human bone marrow mesenchymal stem cells (hBMSCs) were isolated from vertebral body bone marrow aspirates and obtained from donors undergoing spinal fusion with informed written consent and full ethical approval (from Kantonal Ethikkommission Bern 126/03). hBMSCs of two donors were expanded individually and seeded separately, at passage 3, onto the films at a density of 20,000 cells/cm². In order to investigate the biological activity of Dexamethasone released from the composite structures (PTMC/PLA 0, 1 and 2), the cells were cultivated in osteogenic media depleted of any Dexamethasone (called "OM –") based on basic low glucose DMEM (GIBCO) supplemented with 10 % serum (SeraPlus), 1 % penicillin/streptomycin (GIBCO), 50 µg/mL ascorbic acid and 5 mM glycerol-2-phosphate (all from Sigma-Aldrich). The osteogenic differentiation of hBMSCs in the described groups were compared to cells seeded on PTMC/PLA 0, cultivated under non-osteogenic condition (negative control in basal medium, called "BM", based on basic low glucose DMEM supplemented with 10 % serum and 1 % penicillin/streptomycin) and complete osteogenic medium (positive control, called "OM +" similar to "OM –" composition but supplemented with 10 nM Dexamethasone, from Sigma-Aldrich). After seeding, the 96-well plates were filled with 200 µL of the different medium and were changed three times a week for the 28 days of the osteogenic experiment. For all the *in vitro* investigation, control surfaces based on tissue culture polystyrene (TCPS) was used (96 well plate TPP, Trasadingen, Switzerland).

The cytocompatibility of the different composite films and the cell proliferation kinetic was evaluated using CellTiter Blue assay (Promega, Dübendorf,

Switzerland) at 2, 6, 14, 21 and 28 days post-seeding (n=5 per group), following the supplier's recommendation. The resulting fluorescence intensity was read with a multi-plate reader (Viktor³, 1420 Multilabel Count, Perkin-Elmer) and values were corrected using cell-free condition.

For DNA quantification, samples were first incubated in lysis buffer made of Triton X-100 at 0.1 % in 10 mM of Tris-HCl, pH=7.4 (all from Sigma-Aldrich) and followed by one freezing-thawing cycle. Then, DNA amount was estimated using fluorescent CyQuant[®] GR Dye assay, according to the supplier's recommendation (Invitrogen), (n=3 per group). Alkaline phosphatase activity (ALP) from the cell-lysis solution was determined using colorimetric quantification. Briefly, samples along with a set of standard solutions (*p*-nitrophenol of concentrations from 0 to 1,000 μ M) were incubated with alkaline buffer solution (2-amino-2-methylpropanol 1.5 M pH=10.3, from Sigma-Aldrich) and then ALP substrate buffer was added (phosphatase substrate dissolved in diethanolamine buffer at 1 M in 0.5 mM MgCl₂ adjusted pH=9.8). After mixing, and heating (at 37 °C for exactly 15 min), a solution of NaOH at 0.1 M was added to each tube in order to stop the reaction. Then, the intensity of *p*-nitrophenol formation was monitored at 405 nm. The total ALP contents were expressed as enzyme activity units in nmol/min (n=3 per group), as a function of total DNA (ng) per well measured using CyQuant[®] assay. ALP staining was performed after washing the cell monolayers with PBS (3 times), fixation (with ice cold ethanol 90 % for 4 min.), washing with deionised (DI) water and lately, staining with Fast Blue dye solution for 1 h wrapped in tin foil (Naphthol AS-MX, according to Sigma's recommendation). After incubation,

1 samples were washed 3 times with DI water and imaged by light microscopy
2 (MacrofluoTM from Leica).

3 The occurrence of mineralization was detected using Alizarin Red Staining (ARS,
4 Sigma-Aldrich), with TCPS used as control films. The cell monolayer was washed
5 with PBS, fixed with formaldehyde 4 % and further washed with DI water. Then,
6 40 mM ARS solution at pH=4.2 was added to each well for 1 h and thoroughly
7 washed with DI water for 5 days. Finally, samples were imaged by light
8 microscopy (MacrofluoTM from Leica) and a quantification of the ARS was
9 performed by acid extraction thereafter. Briefly, acetic acid (at 10 %) was added to
10 each well for 30 min, and the loosely attached monolayer of cells was transferred
11 to Eppendorf tubes and heated up to 85 °C for 10 min, then placed on ice for 5 min.
12 After centrifugation at 20,000 g for 15 min, ammonium hydroxide was added to
13 the supernatant (final pH of 4.1-4.5) and absorbance was recorded at 405 nm and
14 compared to ARS standard solutions ranged from 0 up to 2,000 µM (n=3 per group)
15 (For all the mentioned assays, background values obtained from cell-free condition
16 are subtracted to the final values).

17 SEM analyses required the fixation of the samples overnight in buffered
18 paraformaldehyde at 4 %, the dehydration with gradual concentration of ethanol up to
19 100 % followed by immersion in hexamethyldisilazane (Sigma-Aldrich). After complete
20 drying, the samples were sputter-coated with C and investigated using a Hitachi S4700
21 FESEM instrument. In order to validate the presence of CaP mineralization by hBMSCs
22 triggered by the release of DEXA from PTMC/PLA films, we carried out energy dispersive
23 X-ray analysis (EDX, Oxford Instruments, UK), following C coating.

Statistical analyses

Statistical analysis of data was performed using Prism software (GraphPad Software, La Jolla, CA, USA). We assumed normal distribution of data. One-way ANOVA with Tukey's multiple comparison test was applied to detect significant differences between experimental groups (with $p < 0.05$). Data presented are means \pm standard deviation (SD) unless stated otherwise.

Results and discussion

Physical properties of the PTMC / PLA hybrid structures

The morphologies of electrospun fibers (with and without Dexa) were characterized using SEM (Figure 1A). The incorporation of Dexa into PLA produced more uniform and smaller fiber dimensions, with an average diameter for PLA fibers decreasing from $1.23 \pm 0.47 \mu\text{m}$ (PLA 0) to $0.39 \pm 0.14 \mu\text{m}$ and $0.74 \pm 0.15 \mu\text{m}$ for PLA 1 and PLA 2, respectively (Figure 1B). Some heterogeneity (*e.g.* beads) was observed on fibers with 0.68 wt% Dexa, which is ascribed to the decreased viscosity of the spinning solution. However, no beads were observed on fibers with 2.42 wt% Dexa, which displayed smooth surfaces. The difference was attributed to the increased solubility of Dexa in methanol (used at higher Dexa concentrations) compared to DMF. Moreover, the formation of larger fibers using methanol (fibers with high drug loading) compared to those formed in DMF (fibers with low drug loading) is explained by the faster evaporation rate of methanol

1 compared to DMF, which resulted in quicker solidification of the fluid jet and
2 reduced fiber stretching.

3 The thermal properties of electrospun fibers were characterized next, using DSC
4 (Figure 2A and B). A melting point (T_m) at 154°C is measured for all samples
5 except for PLA 2 (153°C). The glass transition temperature (T_g) of bulk PLA
6 (63.9°C) was decreased after electrospinning (PLA 0, 60.0°C) and further
7 decreased to 59.2°C (PLA 1) and 59.0°C (PLA 2) respectively upon incorporation
8 of Dexa. The decrease in T_g after electrospinning is caused by the inner stress
9 retained within fibers as a result of jet stretching, which makes molecules become
10 mobile at lower temperatures.³² Small molecules, such as Dexa, are considered to
11 act as plasticizer and further decreased the T_g of PLA, although this transition
12 remained significantly higher than body temperature. Cold crystallization is
13 observed on all electrospun PLA fibers' thermograms. The cold crystallization
14 peak becomes sharper and cold crystallization temperature (T_{cc}) is shifted to lower
15 temperatures (from 95.4°C to 87.9°C) after incorporating 2.42 wt% Dexa. The
16 crystallinity of bulk PLA is decreased from 34.4 % to 3.40 % after electrospinning
17 and further decreased to 2.10 % after adding 0.68 wt% Dexa. However, the
18 crystallinity is increased slightly to 5.70 % when using methanol instead of DMF.
19 The changes in PLA crystallinity are considered to affect the mechanical properties
20 of fibers which were further studied via tensile tests.

21 We next investigated the formation of PTMC/PLA fiber composites. In our
22 previous report,^{17,18} PTMC/PLA fiber composites were prepared by impregnating
23 PTMC/propylene carbonate solution into electrospun PLA fiber mat, followed by
24 UV-crosslink and solvent extraction (for removing propylene carbonate). Based on

the established method, we first integrated icaritin-loaded PLA fibres into PTMC and monitored its *in vitro* release, via HPLC. A representative chromatogram of direct icaritin injection is shown in Figure 3A; an icaritin peak at 3.5 min elution time was observed. However, in the following *in vitro* release assays, no icaritin release was observed from PTMC/PLA fibre composites in contrast to the slow-release of icaritin observed from PLA fibres alone. To verify whether icaritin was physically trapped in PTMC or lost during composite preparation procedure, a series of tests were performed. Firstly, the PTMC/icaritin-loaded fibre composites were incubated in a good solvent, THF, for 24 h. The supernatant was retrieved and analysed using HPLC; no icaritin was detected (a representative chromatogram of supernatant is shown in Figure 3B, in which the icaritin peak disappeared). Secondly, PTMC/PLA fibre composites were incubated in icaritin/THF solution at known-concentration for 24 h. No decrease in icaritin concentration was observed, implying that icaritin does not simply remain trapped in these scaffolds. Thirdly, icaritin was incorporated into PTMC by directly dissolving in PTMC/propylene carbonate solutions. The icaritin-loaded PTMC was extracted by THF, but still no icaritin was observed by HPLC. Hence our data suggested that icaritin was not physically trapped in the composites, but was somehow degraded or trapped during the photopolymerisation process. We further analysed the extracted fractions that were used for the removal of propylene carbonate after polymerisation. No icaritin was detected in these solutions either, indicating that no icaritin was lost during the composite preparation procedure either. We therefore proposed that icaritin was extracted from electrospun fibres into the PTMC/propylene carbonate phase and reacted with methacrylate-ended PTMC macromers during the UV-crosslinking of

the matrix. Hot pressing, a solvent-free composite preparation method, was therefore used for the rest of our work. Indeed, after icaritin-loaded electrospun PLA fibres were incorporated into PTMC, icaritin release was observed and monitored by HPLC (Figure 3C). Therefore, in these conditions, PLA fibres act as a protecting phase for icaritin loading.

The versatility of this approach for the encapsulation of various drugs into UV crosslinked PTMC/PLA fibre composites was further demonstrated by replacing icaritin with Dexa. To investigate the occurrence of cross-reactions between methacrylate end-groups and Dexa, a PEG methacrylate was photo-cured in the presence of Dexa. The molar ratio of methacrylate: Dexa: PI was set at 10:1:1, comparing to that in PTMC composite where methacrylate: Dexa: PI was 10:0.15:1 (for PTMC/PLA 1) and 10:0.5:1 (for PTMC/PLA 2), respectively. Higher Dexa concentration was used to increase signal intensity. The starting materials and resulting products were characterised via GPC. Dexa was identified by its RI signal, at 18.9 min (Figure 4A). The RI signal against elution time of Dexa and PEG-methacrylate before and after UV curing is presented in Figure 4B. After UV curing, the intensity of Dexa peak (eluted at 18.9 min) is significantly reduced. In the meantime, the peak corresponding to PEG-methacrylate (17.9 min) is shifted to lower elution time (17.7 min) with increased signal intensity. The shift of PEG-methacrylate signal peak, the decreased signal intensity of Dexa and the increased signal intensity of PEG-methacrylate constitute further evidence of the coupling between Dexa and PEG-methacrylate. The reaction between Dexa and methacrylate-ended macromers shows the instability of Dexa when exposed to UV-curing processes and its potential deactivation when directly integrated into

methacrylate-based matrices. It is therefore crucial to protect such drugs from exposure of radicals involved in the curing reaction.

Therefore we proposed to use PLA electrospun fibers hot pressed into a PTMC matrix to protect Dexa loaded during photo-crosslinking, to ensure drug's retention and release from the resulting scaffolds under its active form. SEM images of PTMC/PLA fiber composites are presented in Figure 5, where both sample surface and cross-sections are presented. The composite surfaces are covered by PTMC, with some PLA fibers exposed. We observed a good compatibility of the composite structures, as PLA fibers are well wetted by the PTMC matrix and interspaces between fibers are filled by the matrix and resulting in nearly void-free composites (Figure 5). Strong interfacial bonding of PLA fibres to PTMC is evidenced by SEM as most fibers remain well embedded within the matrix upon fracture of the corresponding samples, indicating good levels of interactions between fibers and the surrounding PTMC matrix.

The mechanical properties of both electrospun fibers and PTMC/PLA fiber composites are quantified and the results are presented in Figure 6 and Table 1. It is found that the Young's modulus and strength of electrospun fiber mats is much lower compared to bulk PLA (3.5 GPa, provided by supplier), although electrospun nanofibers (diameter 200-300 nm) were reported to exhibit Young's moduli up to three times that of bulk PLA.⁴³ The reason for this decrease is the combined effect of the porosity of the mats and the lack of orientation of the fibers, allowing fiber-fiber sliding and reorientation during stretching of the mats. PLA 2 displays a higher Young's modulus than PLA 0, presumably due to its higher crystallinity (5.7 % compared to 3.4 %). Meanwhile, PLA 1 exhibits lower failure strain, which

may be explained by its more heterogeneous structure, with the presence of beads in the nano-fibers (see Figure 1A, sample PLA1), which can act as potential defects, resulting in lower failure strains. However, the mechanical properties of PTMC were significantly improved by the addition of electrospun PLA fibers. The Young's moduli of PTMC composites increased by more than one order of magnitude, compared to the simple PTMC matrix, and their tensile strength increased by 3-4 folds; This is an indication of the high reinforcing efficiency of the PLA fibers, as a result of the good integration of the electrospun fibers in the PTMC matrix.

In vitro release of Dexa from electrospun fiber and PTMC/fiber composites

The *in vitro* release profile of Dexa from electrospun fibers and PTMC/PLA fiber composites was examined next, over a period of five weeks, *via* HPLC analysis of the supernatant (Figure 7). All samples showed a quick decrease in their release rate in the first eight days followed by a stable and sustained release profile. PLA 2 exhibited the fastest release rate over the whole test period compared to other samples (initially 1.1×10^{-6} M/day then decreases to 2.0×10^{-9} M/day after five weeks). By incorporating Dexa into PTMC composites, the elution kinetic is effectively reduced by 6-10 folds in the first four days. In comparison, a more stable Dexa release rate is achieved by incorporating PLA 2 into PTMC, for which release concentrations ranged from 1.4×10^{-7} M/day to 6.0×10^{-10} M/day. PLA 1 fibers displayed the slowest initial release but a stable release profile, ranging from

1 4.1×10^{-9} M/day to 2.0×10^{-10} M/day. After integrating them within PTMC, the
2 composites exhibited a faster initial release rate than fibers alone, in the first three
3 days, but a stable release was maintained after ten days. The rapid initial Dexamethasone
4 release from composites is ascribed to the incomplete coverage of PTMC on the
5 fiber surface (see Figure 3).

6 For *in vitro* cell assays (four weeks period), PTMC/PLA fiber composites were
7 used (both low and high Dexamethasone loading (PTMC/PLA 1 and PTMC/PLA 2, compared
8 to drug-free PTMC/PLA 0). According to the release kinetic results obtained
9 (Figure 7), we can extrapolate that the concentrations of Dexamethasone released in the
10 culture media (using composite discs of 1.5 mg incubated in 200 μ L cell culture
11 medium) will range between 9.4×10^{-7} M to 6.5×10^{-9} M for PTMC/PLA 2 and
12 6.4×10^{-7} M to 6.7×10^{-10} M for PTMC/PLA 1, which are in the bioactive
13 concentration windows as previously mentioned.²⁴

14 In addition, after 5 weeks of incubation in PBS, the PTMC/PLA fiber composites
15 were characterized using SEM (see supplementary information Figure SD1). These
16 images clearly indicate that the composite structures were well preserved, with
17 similar features to those initially observed on pristine composites (Figure 5), for
18 both surface and cross-section analysis. We observed that the PLA fibers were still
19 fully embedded within the PTMC matrix, indicating that the hybrid PTMC/PLA
20 fiber structures are morphologically stable during the 5 weeks of experiment.

In vitro differentiation of MSCs triggered by Dexa release from composites

Having confirmed the ability to release Dexa from PTMC/PLA composites, we next examined their potential to be used as carrier of Dexa and to maintain its bioactivity to trigger osteogenic differentiation of MSCs. To this aim, Dexa was selected as drug model as it exhibits a strong "concentration-dependent" biological activity on stem cells. For instance, depending on the charge of Dexa in medium, it can favour *in vitro* hBMSCs proliferation and/or osteogenic differentiation. Both *et al*, showed that cell culture medium supplemented with 10^{-8} M of Dexa promoted both the proliferation and the differentiation of hBMSCs.⁴⁴ However, a reverse effect on hBMSCs has been reported using higher Dexa dosages (*i.e.* 10^{-7} M), with a shift toward adipogenic differentiation associated with a decrease cell proliferation rate⁴⁴⁻⁴⁶). Such biological activity makes Dexa an excellent candidate to validate the control of the release of Dexa enabled by PTMC/PLA hybrid systems.

Two days post-seeding (Figure 8A), no difference in hBMSCs density could be detected between the different groups containing or not Dexa, either in the media or loaded in the films. Indeed, when cells were seeded at a low density of 6,000 cells/well, a 3 to 5 days lag phase was usually observed, before a rapid growth phase is resumed.⁴⁴ This corroborates our results as the effect of Dexa could be first seen at Day 6 (Figure 8B), with significant increase in cell proliferation for all groups containing Dexa. The effective release of Dexa from PTMC/PLA 1 and 2 therefore correlates with an accelerated cell growth for those two groups in comparison to Dexa-free PTMC/PLA 0, in media depleted of any Dexa (OM-),

1 therefore confirming the retention of the activity of DM upon elution from
2 PTMC/PLA scaffolds. Similar conclusions can be drawn for the later time points
3 (Day 14, 21 and 28, Figure 8C, D and E respectively), with superior hBMSCs
4 proliferation on OM+ condition, observed on both PTMC/PLA 0 and controls
5 TCPS, and on PTMC/PLA loaded with Dexa (1 and 2) compared to PTMC/PLA 0
6 even if not systematically significant. At day 21, fluorescence values for the
7 PTMC/PLA 0 and TCPS groups cultivated in OM+ were similar to the PTMC/PLA
8 1 and 2, demonstrating the beneficial effect of Dexa released from the composite
9 films as no significance were observed between PTMC/PLA 0 and TCPS in OM+
10 compared to PTMC/PLA 1 and PTMC/PLA 2. As the cells reached high degrees
11 of confluency following 21 days of cultivation, the fluorescent values measured at
12 Day 28 were not increased compared to previous time-points, but results displayed
13 similar trends (Figure 8E). For all time points, cell proliferation was always the
14 lowest in BM conditions, in agreement with previous results, showing that ascorbic
15 acid is an important stimulator of hBMSCs proliferation, in addition to DEXA.⁴⁷

16 Overall, our results demonstrated that the sustained release of biologically active
17 DEXA from PTMC/PLA scaffolds stimulate hBMSCs proliferation, but without
18 following a concentration-dependent scenario, as values for PTMC/PLA 1 were
19 similar to PTMC/PLA 2 for all time points. Indeed, as shown by the release kinetic
20 presented in Figure 7, the composite structures with the DEXA charges of 0.68 and
21 2.42 wt% release the drug at a concentration below the cytotoxic threshold of 10^{-7}
22 M.^{45,46}

1 It is well known that supplementing media with the synthetic glucocorticoid Dexamethasone
2 at an appropriate dosage induces hBMSCs to differentiate towards osteogenic
3 lineage. One early biochemical marker commonly investigated to validate
4 osteogenic differentiation *in vitro* is alkaline phosphatase (ALP).^{48,49} For both time
5 points investigated (Day 14 and 21, Figure 9A and B, respectively), the ALP
6 activity was negligible on BM condition on both PTMC/PLA 0 and TCPS and on
7 OM- without Dexamethasone. Robust ALP stainings were observed in OM+ conditions, but
8 also for cells growing on PTMC/PLA 1 and 2 substrates (Figure 9C, only shown
9 for donor 1). Hence, the continuous release of Dexamethasone from hybrid films allows to
10 trigger stem cells differentiation, to a similar level to that observed for cells
11 cultured in OM+, where media was constantly refreshed with 10 nM of Dexamethasone, as
12 no significant difference was measured between PTMC/PLA and TCPS in OM +
13 and PTMC/PLA 1 and 2.

14 ALP being an early osteogenic marker, it is not surprising to observe a decline of
15 its activity between Day 14 and Day 21 for some groups (*e.g.* PTMC/PLA 2),
16 revealing that the peak of ALP activity is already passed between those two time
17 points. In fact, PTMC/PLA 2 releasing more Dexamethasone than PTMC/PLA 1 (Figure 7),
18 it is reasonable to hypothesize that the ALP peak occurred earlier in this condition
19 and that, at Day 21, the ALP activity has already decreased again. Such
20 phenomenon was reported in other studies, as during cell maturation ALP naturally
21 decreases and cells start to deposit minerals (calcium and phosphate), considered
22 as a later marker of osteogenic differentiation.⁵⁰ *In vitro* mineralization was
23 monitored in our study using Alizarin Red Staining (ARS) and quantification.

Further indication of osteogenic differentiation of hBMSCs induced by the release of Dexa was evidenced by the staining and quantification of calcium deposition (Figure 10). At both time points investigated (Day 21 and 28), the Dexa-depleted medium, present in the BM and drug-free Dexa PTMC/PLA 0 in OM- conditions, did not permit cells to mineralize their matrix (Figure 10B and C). In contrast, the presence of Dexa either directly supplemented within the medium (in OM+) or diffusing from PTMC/PLA 1 and 2 scaffolds allowed hBMSCs to fully undergo osteogenic differentiation with robust time-dependent biomineralization (Alizarin Red Staining images, Figure 10C). No significance was observed between Ca^{2+} formed in fully supplemented OM media and in the PTMC/PLA 1 and 2 for both time points. In this study, Dexa was selected as a driving source model for osteogenic differentiation. For the positive controls, this factor was directly introduced via the culture medium of hBMSCs (OM+).

This osteogenic study therefore demonstrates that hybrid PLA/PTMC films loaded with Dexa successfully trigger hBMSCs differentiation towards a mature osteoblast lineage, as both early (ALP activity, Figure 9) and late (Ca^{2+} deposition, Figure 10) markers were up-regulated to similar levels to those observed for the positive OM+ condition.

In addition, scanning electron microscopy (SEM) of samples obtained after 28 days of cell culture (Figure 11) corroborated ARS results. We could not detect any clusters of minerals deposited by the hBMSCs on the control groups (cells cultivated in the absence of Dexa, *i.e.* PTMC/PLA 0 in BM and in OM-), whereas numerous inorganic clusters (supposedly CaP) could be distinguished for the positive control (OM+) and on Dexa-

loaded composite films (PTMC/PLA 1 and 2). Further EDX analyses confirmed the presence of Ca and P elements in the peri-cellular regions of hBMSCs cultivated on Dexamethasone-loaded film (Figure SD3). Therefore, SEM images confirm the potential of Dexamethasone-loaded PTMC/PLA composite films to stimulate stem cells differentiation and to promote the deposition of minerals, essential for the application of these matrices in bone tissue engineering.

Conclusion

In this study, biocompatible and degradable polymeric composites based on electrospun PLA fibers and photo-crosslinked PTMC were successfully fabricated. The fibers were incorporated into PTMC macromer using a hot-pressing method followed by UV-curing. The composites exhibited significant improvements in mechanical performance compared to neat PTMC. The incorporation of PLA fibers permits to increase the PTMC's Young's modulus by one-order of magnitude and its tensile strength by 3-folds. The PLA fibers showed strong interfacial bonding with PTMC matrix (no fiber pull-out was observed for cold-fractured composites) and physical stability was observed, even after 5 weeks of *in vitro* incubation. Dexamethasone was loaded into composites by first co-electrospinning with PLA and then integration into the PTMC matrix. Using this approach, the UV-triggered cross-reaction between Dexamethasone and methacrylate-terminated PTMC macromers was avoided. Thus the biological activity of Dexamethasone integrated in such polymer-polymer composite structure was preserved. Moreover, the combination of electrospun

fibers with PTMC matrix also achieved a stable and sustained Dexa release profile, which allowed the improvement of hBMSCs proliferation and osteogenic differentiation. Overall, the concept of polymer/polymer hybrid structures offers a high degree of versatility as various therapeutics, especially those known to react with photo-crosslinking reaction, can be loaded in the corresponding scaffolds. This study demonstrates the potential of polymer-polymer scaffolds to simultaneously reinforce the mechanical properties of soft matrices and to load sensitive drugs in scaffolds that can be fabricated *via* additive manufacturing.

Acknowledgement

The authors acknowledge the funding provided by NSFC-DG-RTD Joint Scheme (Project No. 51361130034), the RAPIDOS project under the European Union's 7th Framework Programme (Project No. 604517) and Dr. Christoph Sprecher for his technical expertise on EDX.

Disclosure

The author reports no conflicts of interest in this work.

Reference

1. Fukushima K. Poly(trimethylene carbonate)-based polymers engineered for biodegradable functional biomaterials. *Biomater Sci.* 2015;4(1):9-24.
2. Zhang Z, Kuijer R, Bulstra SK, Grijpma DW, Feijen J. The in vivo and in vitro degradation behavior of poly(trimethylene carbonate). *Biomaterials.* 2006;27(9):1741-1748.

- 1 3. Rongen JJ, van Bochove B, Hannink G, Grijpma DW, Buma P. Degradation
2 behavior of, and tissue response to photo-crosslinked poly(trimethylene carbonate)
3 networks. *J Biomed Mater Res A*. 2016;104(11):2823-2832.
- 4 4. Pêgo AP, Grijpma DW, Feijen J. Enhanced mechanical properties of 1,3-
5 trimethylene carbonate polymers and networks. *Polymer*. 2003;44(21):6495-6504.
- 6 5. Qin Y, Yang J, Xue J. Characterization of antimicrobial poly(lactic
7 acid)/poly(trimethylene carbonate) films with cinnamaldehyde. *J Mater Sci*.
8 2014;50(3):1150-1158.
- 9 6. van Leeuwen AC, Bos RR, Grijpma DW. Composite materials based on
10 poly(trimethylene carbonate) and beta-tricalcium phosphate for orbital floor and
11 wall reconstruction. *J Biomed Mater Res B, Appl Biomater*. 2012;100(6):1610-
12 1620.
- 13 7. Guillaume O, Geven MA, Grijpma DW, et al. Poly(trimethylene carbonate) and
14 nano-hydroxyapatite porous scaffolds manufactured by stereolithography. *Polym*
15 *Adv Technol*. 2016;28(10):1219-1225.
- 16 8. Guerin W, Helou M, Carpentier J-F, Slawinski M, Brusson J-M, Guillaume SM.
17 Macromolecular engineering viaring-opening polymerization (1):l-
18 lactide/trimethylene carbonate block copolymers as thermoplastic elastomers.
19 *Polym Chem*. 2013;4(4):1095-1106.
- 20 9. Yang L-Q, He B, Meng S, et al. Biodegradable cross-linked poly(trimethylene
21 carbonate) networks for implant applications: Synthesis and properties. *Polymer*.
22 2013;54(11):2668-2675.
- 23 10. Schuller-Ravoo S, Feijen J, Grijpma DW. Flexible, elastic and tear-resistant
24 networks prepared by photo-crosslinking poly(trimethylene carbonate)
25 macromers. *Acta Biomater*. 2012;8(10):3576-3585.
- 26 11. Guillaume O, Geven MA, Sprecher CM, et al. Surface-enrichment with
27 hydroxyapatite nanoparticles in stereolithography-fabricated composite polymer
28 scaffolds promotes bone repair. *Acta Biomater*. 2017;54:386-398.
- 29 12. Bose S, Vahabzadeh S, Bandyopadhyay A. Bone tissue engineering using 3D
30 printing. *Mater Today*. 2013;16(12):496-504.

- 1 13. Blanquer SBG, Werner M, Hannula M, et al. Surface curvature in triply-periodic
2 minimal surface architectures as a distinct design parameter in preparing advanced
3 tissue engineering scaffolds. *Biofabrication*. 2017;9(2):025001.
- 4 14. Jansen J, Boerakker MJ, Heuts J, Feijen J, Grijpma DW. Rapid photo-crosslinking
5 of fumaric acid monoethyl ester-functionalized poly(trimethylene carbonate)
6 oligomers for drug delivery applications. *J Control Release*. 2010;147(1):54-61.
- 7 15. ter Boo GA, Grijpma DW, Richards RG, Moriarty TF, Eglin D. Preparation of
8 gentamicin dioctyl sulfosuccinate loaded poly(trimethylene carbonate) matrices
9 intended for the treatment of orthopaedic infections. *Clin Hemorheol Microcirc*.
10 2015;60(1):89-98.
- 11 16. Neut D, Kluin OS, Crielaard BJ, van der Mei HC, Busscher HJ, Grijpma DW. A
12 biodegradable antibiotic delivery system based on poly-(trimethylene carbonate)
13 for the treatment of osteomyelitis. *Acta Orthop*. 2009;80(5):514-519.
- 14 17. Zhang X, Geven MA, Grijpma DW, Gautrot JE, Peijs T. Polymer-polymer
15 composites for the design of strong and tough degradable biomaterials. *Mater*
16 *Today Commun*. 2016;8:53-63.
- 17 18. Zhang X, Geven MA, Grijpma DW, Peijs T, Gautrot JE. Tunable and processable
18 shape memory composites based on degradable polymers. *Polymer*.
19 2017;122:323-331.
- 20 19. Tavakoli-darestani R, Manafi-rasi A, Kamrani-rad A. Dexamethasone-loaded
21 hydroxyapatite enhances bone regeneration in rat calvarial defects. *Mol Biol Rep*.
22 2014;41(1):423-428.
- 23 20. Qiu K, Chen B, Nie W, et al. Electrophoretic Deposition of Dexamethasone-
24 Loaded Mesoporous Silica Nanoparticles onto Poly(L-Lactic Acid)/Poly(epsilon-
25 Caprolactone) Composite Scaffold for Bone Tissue Engineering. *ACS Appl Mater*
26 *Interfaces*. 2016;8(6):4137-4148.
- 27 21. Bordag N, Klie S, Jurchott K, et al. Glucocorticoid (dexamethasone)-induced
28 metabolome changes in healthy males suggest prediction of response and side
29 effects. *Sci Rep*. 2015;5:15954.
- 30 22. Pittenger MF, Mackay AM, Beck SC, et al. Multilineage Potential of Adult
31 Human Mesenchymal Stem Cells. *Science*. 1999;284(5411):143-147.

23. Jaiswal N, Haynesworth SE, Caplan AI, Bruder SP. Osteogenic differentiation of purified, culture-expanded human mesenchymal stem cells in vitro. *J Cell Biochem.* 1997;64(2):295-312.
24. Costa PF, Puga AM, Diaz-Gomez L, Concheiro A, Busch DH, Alvarez-Lorenzo C. Additive manufacturing of scaffolds with dexamethasone controlled release for enhanced bone regeneration. *Int J Pharm.* 2015;496(2):541-550.
25. Huang J, Yuan L, Wang X, Zhang TL, Wang K. Icaritin and its glycosides enhance osteoblastic, but suppress osteoclastic, differentiation and activity in vitro. *Life Sci.* 2007;81(10):832-840.
26. Astolfi L, Guaran V, Marchetti N, et al. Cochlear implants and drug delivery: In vitro evaluation of dexamethasone release. *J Biomed Mater Res B Appl Biomater.* 2014;102(2):267-273.
27. Kim DH, Martin DC. Sustained release of dexamethasone from hydrophilic matrices using PLGA nanoparticles for neural drug delivery. *Biomaterials.* 2006;27(15):3031-3037.
28. Webber MJ, Matson JB, Tamboli VK, Stupp SI. Controlled release of dexamethasone from peptide nanofiber gels to modulate inflammatory response. *Biomaterials.* 2012;33(28):6823-6832.
29. Li L, Zhou G, Wang Y, Yang G, Ding S, Zhou S. Controlled dual delivery of BMP-2 and dexamethasone by nanoparticle-embedded electrospun nanofibers for the efficient repair of critical-sized rat calvarial defect. *Biomaterials.* 2015;37:218-229.
30. Jiang K, Weaver JD, Li Y, Chen X, Liang J, Stabler CL. Local release of dexamethasone from macroporous scaffolds accelerates islet transplant engraftment by promotion of anti-inflammatory M2 macrophages. *Biomaterials.* 2017;114:71-81.
31. Hu X, Liu S, Zhou G, Huang Y, Xie Z, Jing X. Electrospinning of polymeric nanofibers for drug delivery applications. *J Control Release.* 2014;185:12-21.
32. Cui W, Li X, Zhu X, Yu G, Zhou S, Weng J. Investigation of drug release and matrix degradation of electrospun poly (DL-lactide) fibers with paracetamol inoculation. *Biomacromolecules.* 2006;7(5):1623-1629.

33. Zeng J, Yang L, Liang Q, et al. Influence of the drug compatibility with polymer solution on the release kinetics of electrospun fiber formulation. *J Control Release*. 2005;105(1-2):43-51.
34. Huang ZM, He CL, Yang A, et al. Encapsulating drugs in biodegradable ultrafine fibers through co-axial electrospinning. *J Biomed Mater Res A*. 2006;77(1):169-179.
35. Yu D-G, Chian W, Wang X, Li X-Y, Li Y, Liao Y-Z. Linear drug release membrane prepared by a modified coaxial electrospinning process. *J Membr Sci*. 2013;428:150-156.
36. Hu C, Liu S, Zhang Y, et al. Long-term drug release from electrospun fibers for in vivo inflammation prevention in the prevention of peritendinous adhesions. *Acta Biomater*. 2013;9(7):7381-7388.
37. Zheng F, Wang S, Wen S, Shen M, Zhu M, Shi X. Characterization and antibacterial activity of amoxicillin-loaded electrospun nano-hydroxyapatite/poly(lactic-co-glycolic acid) composite nanofibers. *Biomaterials*. 2013;34(4):1402-1412.
38. Yohe ST, Colson YL, Grinstaff MW. Superhydrophobic materials for tunable drug release: using displacement of air to control delivery rates. *J Am Chem Soc*. 2012;134(4):2016-2019.
39. Fan Z, Fu M, Xu Z, et al. Sustained Release of a Peptide-Based Matrix Metalloproteinase-2 Inhibitor to Attenuate Adverse Cardiac Remodeling and Improve Cardiac Function Following Myocardial Infarction. *Biomacromolecules*. 2017;18(9):2820-2829.
40. Geven MA, Varjas V, Kamer L, et al. Fabrication of patient specific composite orbital floor implants by stereolithography. *Polym Adv Technol*. 2015;26(12):1433-1438.
41. Williams CG, Malik AN, Kim TK, Manson PN, Elisseff JH. Variable cytocompatibility of six cell lines with photoinitiators used for polymerizing hydrogels and cell encapsulation. *Biomaterials*. 2005;26(11):1211-1218.
42. Mathew AP, Oksman K, Sain M. The effect of morphology and chemical characteristics of cellulose reinforcements on the crystallinity of polylactic acid. *J Appl Polym Sci*. 2006;101(1):300-310.

43. Naraghi M, Arshad SN, Chasiotis I. Molecular orientation and mechanical property size effects in electrospun polyacrylonitrile nanofibers. *Polymer*. 2011;52(7):1612-1618.
44. Both SK, van der Muijsenberg AJ, van Blitterswijk CA, de Boer J, de Bruijn JD. A rapid and efficient method for expansion of human mesenchymal stem cells. *Tissue Eng*. 2007;13(1):3-9.
45. Walsh S, Jordan GR, Jefferiss C, Stewart K, Beresford JN. High concentrations of dexamethasone suppress the proliferation but not the differentiation or further maturation of human osteoblast precursors in vitro: relevance to glucocorticoid-induced osteoporosis. *Rheumatology (Oxford, U.K.)*. 2001;40(1):74-83.
46. Wang GJ, Cui Q, Balian G. The Nicolas Andry award. The pathogenesis and prevention of steroid-induced osteonecrosis. *Clin Orthop Relat Res*. 2000(370):295-310.
47. Choi K-M, Seo Y-K, Yoon H-H, et al. Effect of ascorbic acid on bone marrow-derived mesenchymal stem cell proliferation and differentiation. *J Biosci Bioeng*. 2008;105(6):586-594.
48. Jaiswal N, Haynesworth SE, Caplan AI, Bruder SP. Osteogenic differentiation of purified, culture-expanded human mesenchymal stem cells in vitro. *J Cell Biochem*. 1997;64(2):295-312.
49. Mendes SC, Tibbe JM, Veenhof M, et al. Relation between in vitro and in vivo osteogenic potential of cultured human bone marrow stromal cells. *J Mater Sci Mater Med*. 2004;15(10):1123-1128.
50. Birmingham E, Niebur GL, McHugh PE, Shaw G, Barry FP, McNamara LM. Osteogenic differentiation of mesenchymal stem cells is regulated by osteocyte and osteoblast cells in a simplified bone niche. *Eur Cell Mater*. 2012;23:13-27.

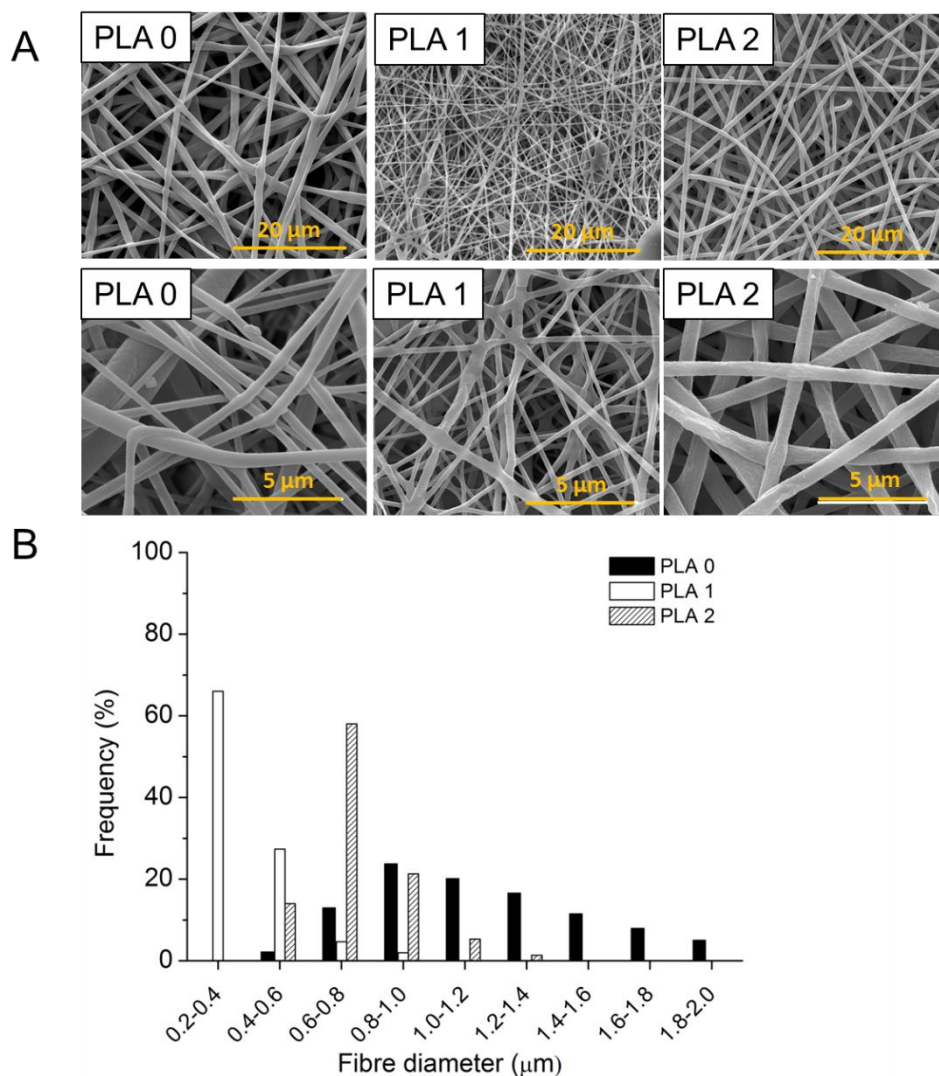


Figure 1: Loading Dexa in PLA results in homogenous and smooth PLA electrospun fibers. (A) SEM images of electrospun fibers; (B) fiber diameter distribution of PLA 0, PLA 1 and PLA 2.

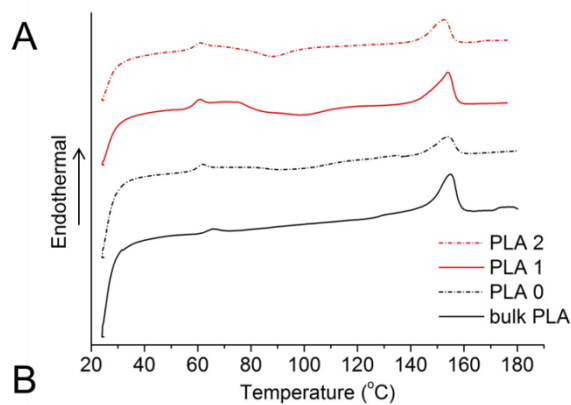


Figure 2: PLA processing and drug loading influence the crystallinity of the electrospun nanofibers. DSC thermograms of the different PLA materials without Dexa (bulk PLA and PLA 0) and with Dexa loading (PLA 1 and 2) (A). Quantification of the PLA fibers thermal properties, depending on the processing method and presence of Dexa (B).

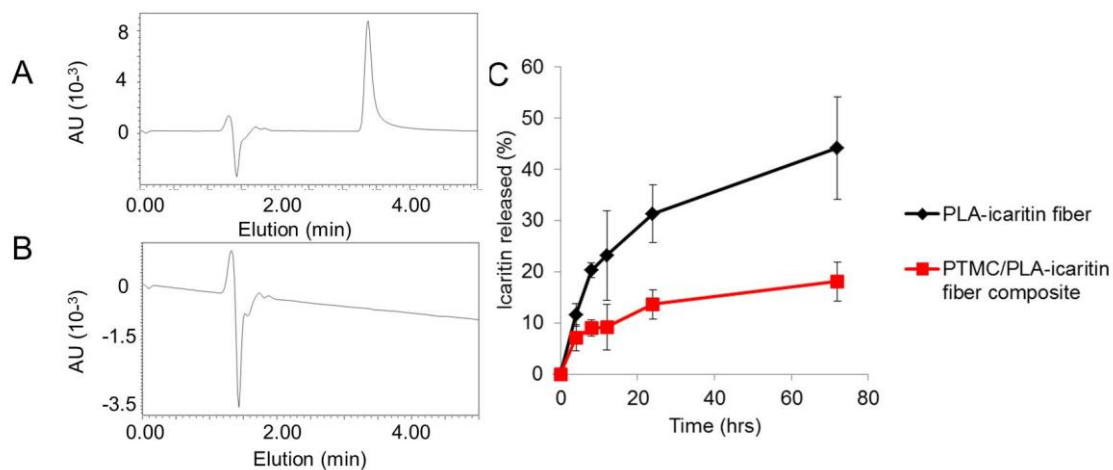


Figure 3: Representative chromatogram of (A) direct icaritin injection and (B) THF extractant of PTMC/icaritin-loaded fiber composite; (C) release profile of icaritin from electrospun fiber (black) and hot-pressed PTMC/PLA fiber composite (red).

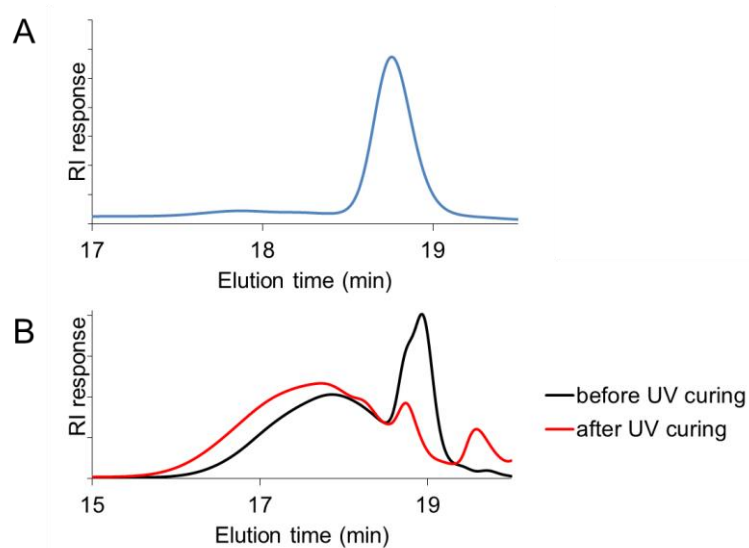


Figure 4: If unprotected, Dexa reacts with methacrylated macromere during UV-reaction. RI signal against elution time of Dexamethasone (A); RI signal against elution time of DEXA and PEG-methacrylate before (black) and after (red) UV curing (B).

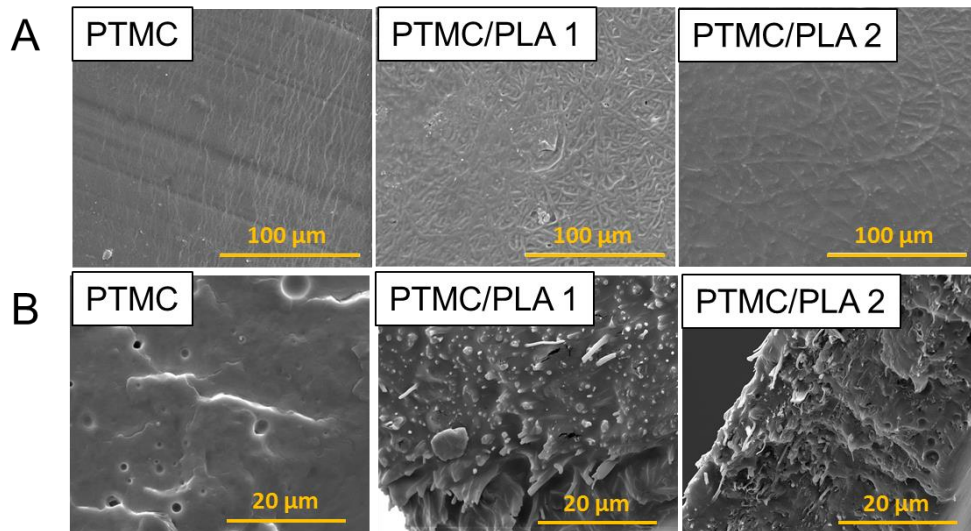


Figure 5: PLA nanofibers exhibit a good physical interaction in hybrid PTMC/PLA structures. SEM images of (A) sample's surface and (B) sample's cross-section.

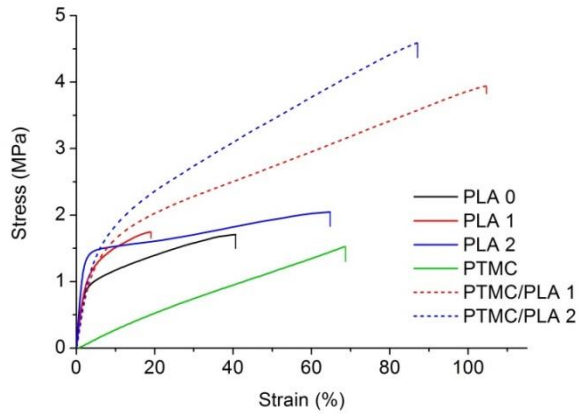


Figure 6: Incorporating PLA nanofibers into PTMC films dramatically improves materials mechanical resistance. Representative stress-strain curve of electrospun fiber mat and PTMC/PLA fiber composites

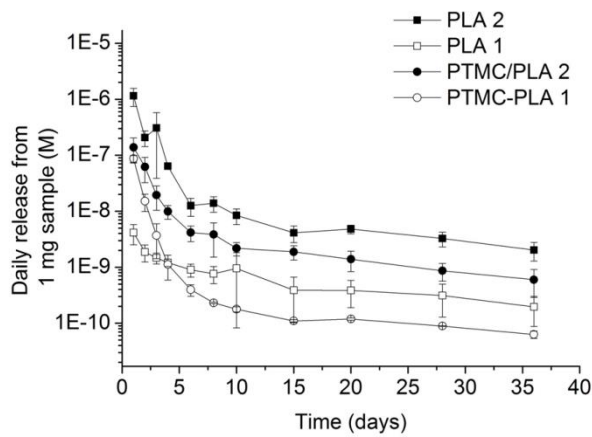
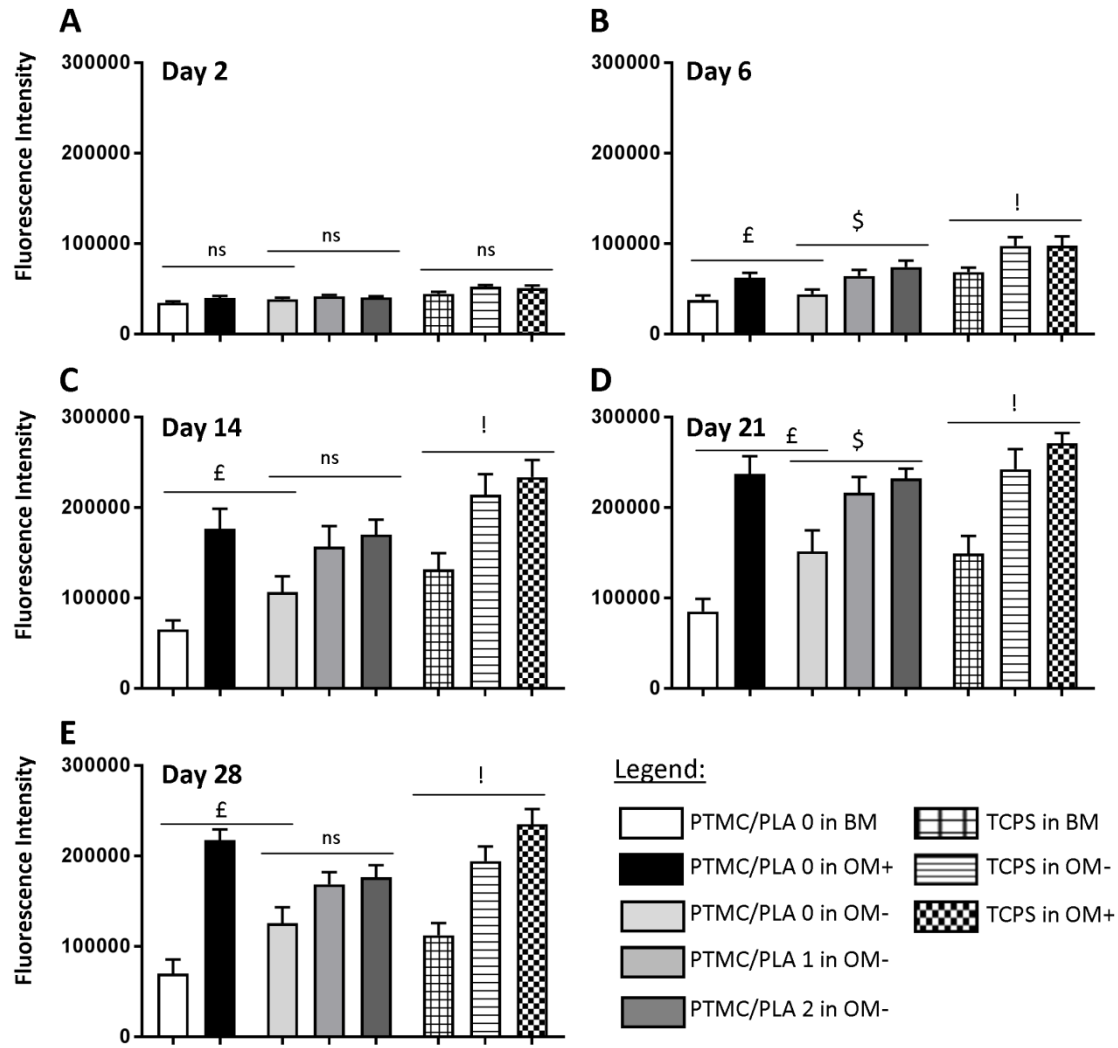


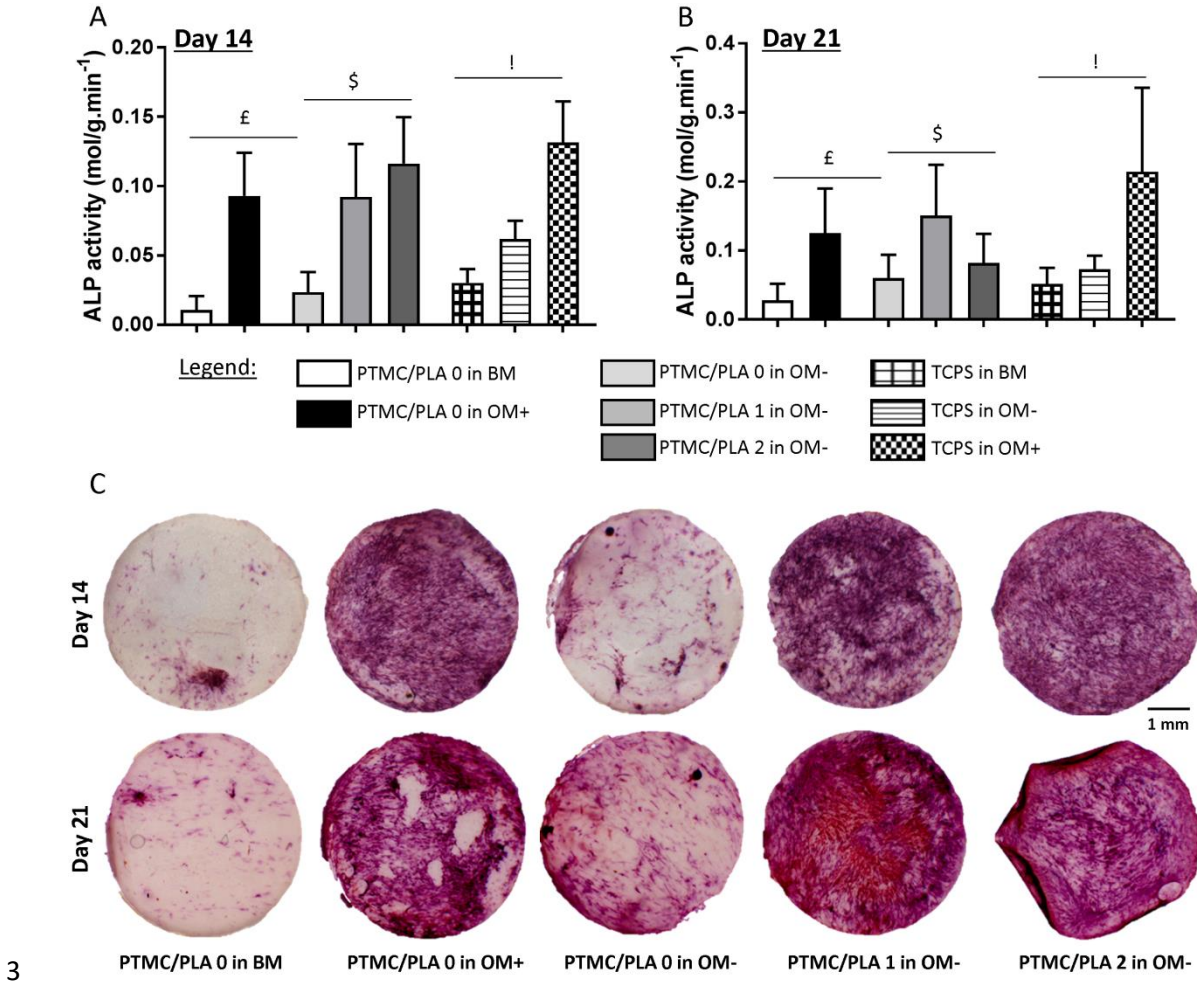
Figure 7: Hybrid films are characterized by a sustained and prolonged release of Dexa.

1 Dexamethasone concentrations released daily from electrospun fibers and PTMC/PLA
2 fiber composites (per 1.0 mg sample in 1.0 mL PBS at 37°C, values presented are non-
3 cumulative).



5 **Figure 8:** Dexa released from PTMC/PLA composite films impacts on hBMSCs
6 proliferation. CellTiter Blue quantification of hBMSCs proliferating on the different
7 substrates in various medium (BM, OM- and OM+) on day 2 (A), day 6 (B), day 14 (C),
8 day 21 (D) and day 28 (E). £ reports significance for drug-free PTMC/PLA 0 regarding
9 the nature of the medium, \$ reports significance for drug-loaded PTMC/PLA on OM-

1 medium and ! reports significance for TCPS regarding the nature of the medium. ns
2 reports non-significance.



3 **Figure 9:** Dexa released from hybrid PTMC/PLA structures recreates in vitro similar
4 condition than osteogenic media on hBMSCs ALP activity. ALP activity measured on day
5 14 and day 21 (A and B respectively, £ reports significance for drug-free PTMC/PLA 0
6 regarding the nature of the medium, \$ reports significance for drug-loaded PTMC/PLA
7 on OM- medium and ! reports significance for TCPS regarding the nature of the medium).
8 ALP staining on hBMSCs monolayer cultivated on the diverse substrates (only shown for
9 1 donor, but similar staining was obtained for both donor, C).

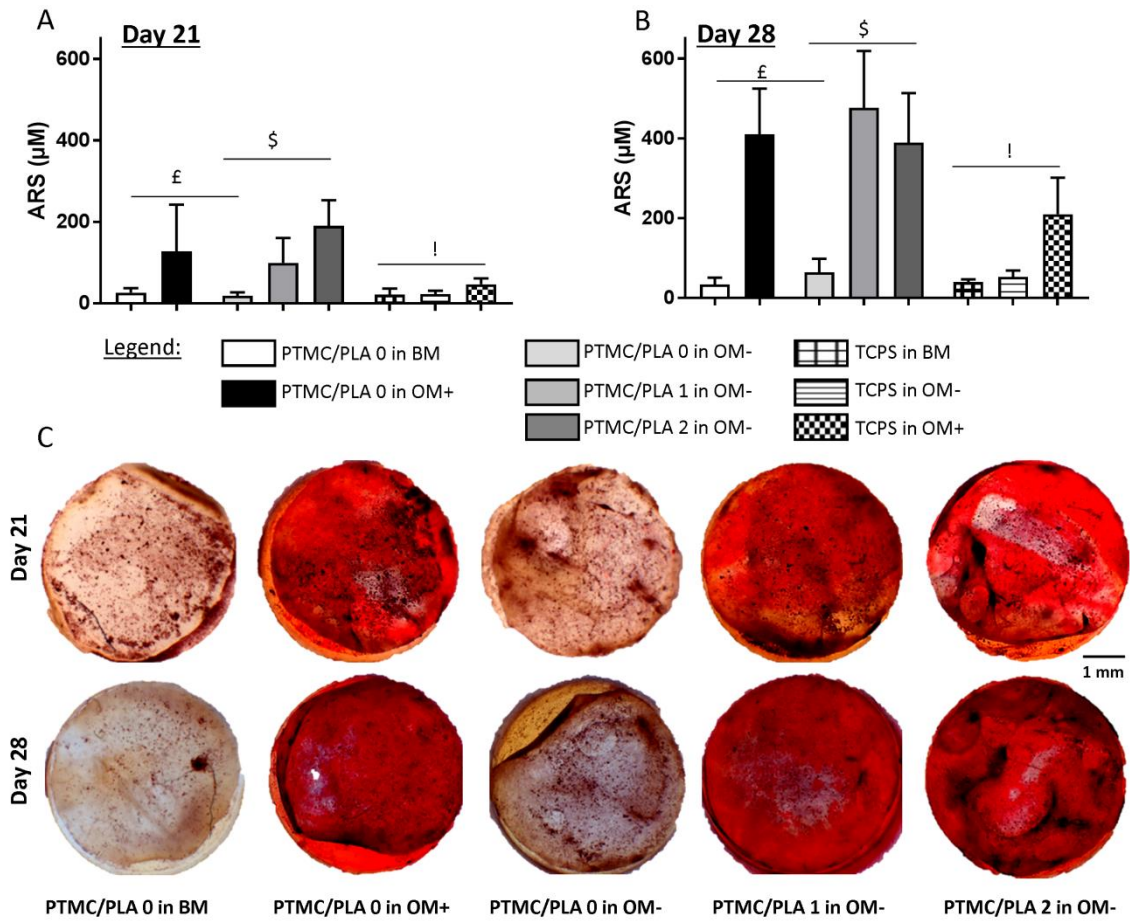


Figure 10: DEXA loaded PTMC/PLA film successfully triggers hBMSCs differentiation towards mineralizing osteoblast-cell lineage. Calcium deposition from hBMSCs was measured on day 21 and day 28 (A and B respectively, £ reports significance for drug-free PTMC/PLA 0 regarding the nature of the medium, \$ reports significance for drug-loaded PTMC/PLA on OM- medium and ! reports significance for TCPS regarding the nature of the medium). Alizarin Red Staining of Ca^{2+} secreted by hBMSCs cultivated on the diverse substrates (only shown for 1 donor, but similar staining was obtained for both donor, C).

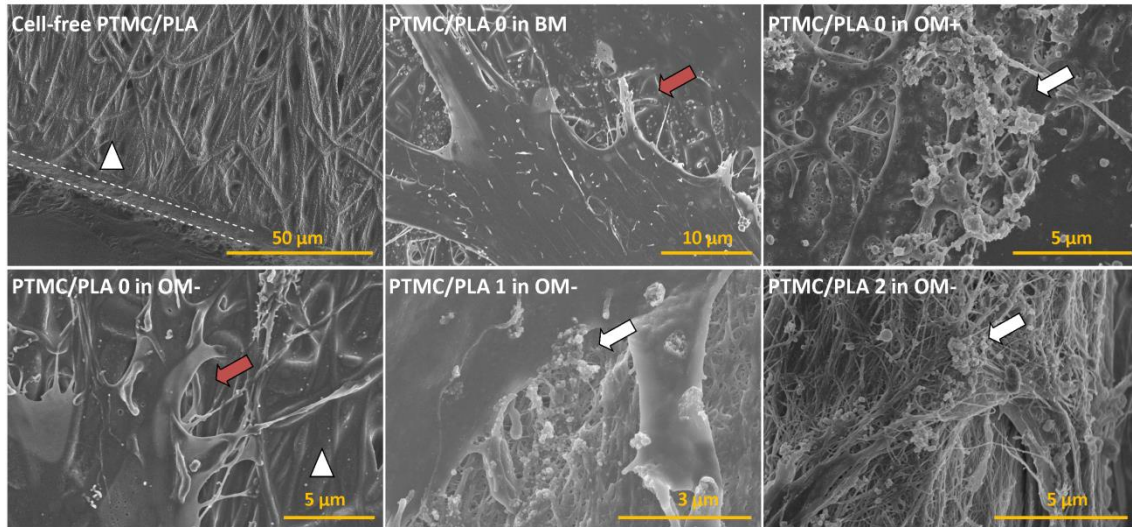


Figure 11: Biomineralization is visible on cell monolayers cultivated on Dexamethasone-loaded films like in OM+ condition. Illustration of PTMC/PLA composite film surface (dash lines denoted the cross-section and white triangle the PLA fibers). The red and white arrows denoted cells' membrane and clusters of minerals respectively. SEM were realized Day 28 of the in vitro culture experiment.

1 **Table 1:** Results of the stress-strain test of electrospun fiber mats and PTMC/PLA fiber
2 composites

Sample	Young's modulus (MPa)	Strength (MPa)	Failure strain (%)
PLA 0	45.32±5.45	2.31±0.94	50.42±27.23
PLA 1	49.66±5.30	2.14±0.36	20.68±4.61
PLA 2	65.89±21.98	2.18±0.82	72.34±6.85
PTMC	2.73±0.48	1.31±0.43	62.17±11.42
PTMC/PLA 1	30.92±6.80	4.61±1.19	106.85±9.78
PTMC/PLA 2	33.96±19.33	3.86±1.41	81.97±13.17

3

4